NANO LETTERS

pubs.acs.org/NanoLett Letter

Distinctive Dielectric Permittivity of Hierarchical Nanostructures with Ordered Nanoparticle Networks Self-Assembled from AB-*g*-NP/AC Block Copolymer Mixtures

Zhanwen Xu, Jiaping Lin,* Liangshun Zhang, and Liquan Wang

Cite This: *Nano Lett.* 2021, 21, 2982−2988 Read Online

ACCESS | Metrics & More | Article Recommendations | Supporting Information

ABSTRACT: Directing nanoparticles into ordered organization in polymer matrix to improve macroscopic properties of nanocomposites remains a challenge. Herein, by means of theoretical simulations, we show the high permittivity of hybrid nanostructures designed with mixtures of AB block copolymer-grafted nanoparticles and lamella-forming AC diblock copolymers. The grafted nanoparticles self-assemble into parallel stripes or highly ordered networks in the lamellae of the AC diblock copolymers. The ordered nanoparticle networks, including honeycomb-like and kagomé networks, provide bending and conductive pathways for concentrating electric fields, which results in the improvement of the permittivity. We envisage that this strategy will open a gateway to prepare hierarchically ordered functional nanocomposites with distinctive dielectric properties.

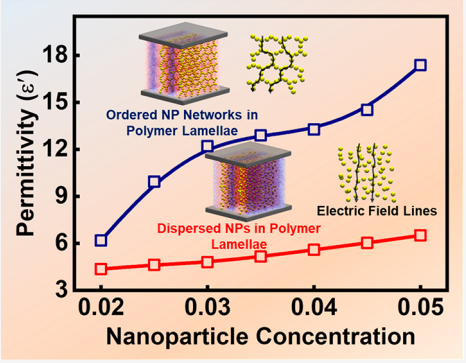

KEYWORDS: *block copolymer-grafted nanoparticles, hierarchical hybrid nanostructures, ordered nanoparticle networks, self-assembly, dielectric permittivity*

Materials with high permittivity are highly desired for practical applications such as dielectric capacitors, energy storage devices, and electromagnetic wave absorbers.[1−4] Polymer nanocomposites containing inorganic nanoparticles (NPs) are one of the promising candidates for these applications, and their permittivity is strongly dependent on the organization of the nanoparticles.[5−8] For example, Luo et al. successfully constructed 3D-$BaTiO_3$ nanoparticle networks in polymer matrix and achieved high permittivity.[9] However, precisely directing nanoparticles into ordered organization in polymer templates to improve the permittivity still remains a challenge, due to the limited understanding of the correlation between the nanostructures and permittivity.

Block copolymers (BCPs) can self-assemble into various ordered nanostructures, which are ideal templates for directing nanoparticle organization and enhancing permittivity.[10−14] However, due to attractive van der Waals and depletion forces, the nanoparticles tend to form aggregates in the polymer matrix. To prevent nanoparticle agglomeration, the nanoparticles are stabilized by grafting polymeric chains, typically homopolymers.[15−17] For example, Lin et al. fabricated nanostructured composites based on PS-*b*-PMMA diblock copolymers and PS-functionalized $BaTiO_3$ NPs.[17] Periodic PS nanocylinders containing PS functionalized $BaTiO_3$ NPs were obtained, and the resulting composites exhibited a high dielectric constant. But the homopolymer-grafted nanoparticles were not well organized in the block copolymer nanodomains and the improvement in the permittivity was limited. Recently, block copolymer-grafted nanoparticles (BNPs) have emerged as novel assembly building blocks.[18−22] For example, Leffler et al. investigated the self-assembly of BNP thin films prepared from poly(styrene-*b*-isoprene) (PS-PI) block copolymers and Cu_2ZnSnS_4 nanoparticles.[23] They found that the BNPs, unlike the homopolymer-grafted nanoparticles, can self-assemble into highly ordered stripes under the confinement of thin films. Inspired by these findings, we expect that the BNPs confined in the block copolymer nanodomains could organize in a highly ordered manner and give rise to high permittivity. However, the self-assembly of BNPs in block copolymer melts has rarely been reported, and the correlation between the nanostructures and the functional properties for the mixture systems is unclear.

Theoretical simulations have been shown to be a powerful tool to study the self-assembly behaviors and dielectric properties of polymer/nanoparticle mixtures.[8,24−27] A series of simulation methods, such as self-consistent field theory/density functional theory,[11,28] molecular dynamics,[15,29] and

Received: January 11, 2021
Revised: March 26, 2021
Published: April 1, 2021

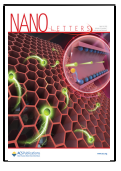

https://doi.org/10.1021/acs.nanolett.1c00122
Nano Lett. 2021, 21, 2982−2988

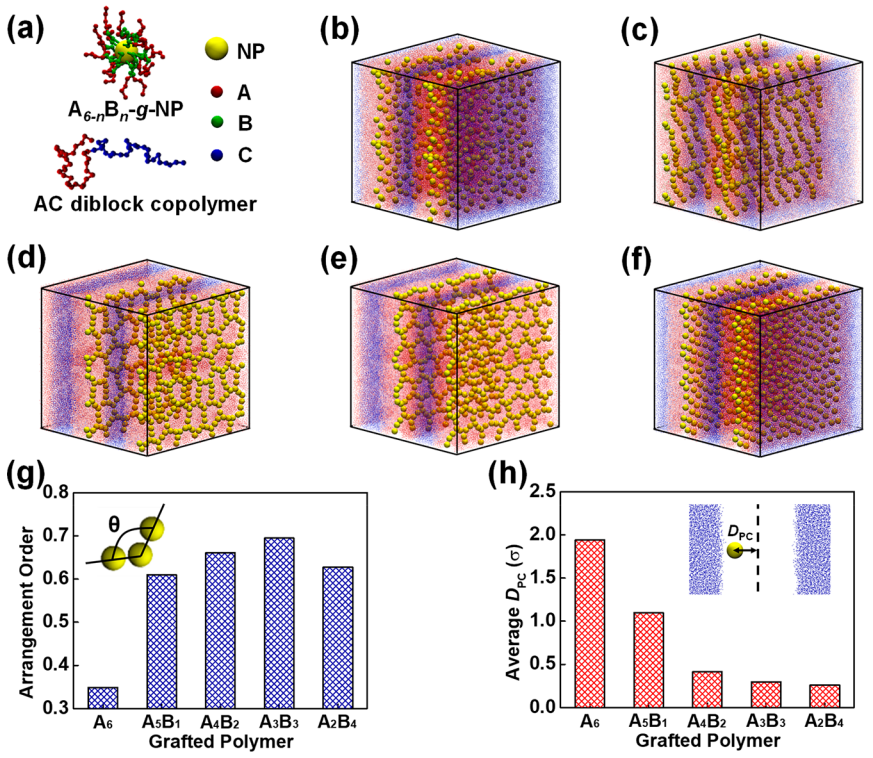

Figure 1. (a) Model of the $A_{6-n}B_n$ diblock copolymer-grafted nanoparticle and the AC diblock copolymer. The nanostructures self-assembled from mixtures of (b) A_6-*g*-NP/AC, (c) A_5B_1-*g*-NP/AC, (d) A_4B_2-*g*-NP/AC, (e) A_3B_3-*g*-NP/AC, and (f) A_2B_4-*g*-NP/AC, at a nanoparticle concentration of $\varphi_P = 0.04$. The yellow, red, and blue colors in the structural snapshots represent the NPs, A blocks, and C blocks, respectively. The B blocks are not shown. (g) Arrangement order parameter of nanoparticles in the nanostructures formed by $A_{6-n}B_n$-*g*-NP/AC with various *n*. The inset shows the angle formed by three neighboring nanoparticles. (h) Average distance between the nanoparticles and the center of the A domains (D_{PC}) in the nanostructures with various *n*. The inset shows the definition of the D_{PC}.

dissipative particle dynamics,[10] were developed to study the nanostructures of polymer/nanoparticle mixtures. To evaluate the effective dielectric properties of nanostructures, a method of finite difference quasielectrostatic modeling has been developed.[27,30,31] This quasistatic method is useful for simulating systems in which the characteristic structures are much smaller than the electromagnetic wavelength.

Herein, we propose a multiscale approach coupling coarse-grained molecular dynamics (CGMD) and finite difference quasielectrostatic modeling to investigate the correlation between the nanostructures and dielectric permittivity of BNP/BCP mixtures. Several hierarchically ordered nanostructures with ordered nanoparticle stripes or networks in the block copolymer matrix are predicted through CGMD simulations. The calculations for the permittivity properties demonstrate that a significant improvement in the permittivity can be obtained when hierarchical nanostructures with ordered nanoparticle networks are formed. The permittivity improvement is a result of concentrated electric fields near the nanoparticle networks. We expect this work to provide useful information for the design and fabrication of advanced functional polymer nanocomposites with high permittivity.

Self-Assembled Nanostructures of AB-*g*-NP/AC. We consider a mixture system containing AB diblock copolymer-grafted nanoparticles (AB-*g*-NPs) and AC diblock copolymers. To predict the self-assembly behavior of the AB-*g*-NP/AC mixtures, a coarse-grained model is constructed in the CGMD simulations, as illustrated in Figure 1a. The AC diblock copolymers are modeled as linear chains of 60 coarse-grained Lennard-Jones (LJ) beads with diameter σ, where σ denotes the LJ unit length. Each coarse-grained bead represents a cluster of monomers. The volume fraction of block A of the AC diblock copolymers is fixed at 0.5. The nanoparticles are represented by LJ spheres of diameter $D = 3\sigma$. Twenty AB diblock copolymers are uniformly tethered onto the surfaces of each nanoparticle via using the maximal volume arrangement of points on the sphere.[32] To ensure the immobilization of the tethered points, we set the nanoparticle and the beads of grafting points as rigid bodies. Each AB diblock copolymer contains 6 LJ beads, i.e., the numbers of beads of block A and B are $6 - n$ and n, respectively (n varies from 0 to 4). We set the masses of the polymer beads and nanoparticles as m and $(D/\sigma)^3 m$ (m denotes the LJ unit mass). Full details of the CGMD method are provided in section 1 of the Supporting Information.

We begin by considering the effect of the graft composition f_B on the self-assembled nanostructures of the $A_{6-n}B_n$-*g*-NP/AC mixtures at a nanoparticle concentration of $\varphi_P = 0.04$. f_B is varied from 0 to 0.66 corresponding to an increase in the bead number of block B (n) from 0 to 4. As shown in Figure 1b–f, the AC diblock copolymers self-assemble into lamellar nanostructures. From Figure 1b, it can be observed that the homopolymer-grafted nanoparticles (A_6-*g*-NP) are organized in a disordered manner in the domains formed by the A blocks. When the grafted homopolymers are replaced by block copolymers, the nanoparticles assemble into ordered nanostructures. Figure 1c–f shows the self-assembled nanostructures of the $A_{6-n}B_n$-*g*-NP/AC mixtures with $n > 0$. When the nanoparticles are grafted with A_5B_1 diblock copolymers, they form parallel stripes in the A domains (Figure 1c). With longer

https://doi.org/10.1021/acs.nanolett.1c00122
Nano Lett. 2021, 21, 2982−2988

B blocks, the A_4B_2-*g*-NPs and A_3B_3-*g*-NPs form ordered networks (Figure 1d and Figure 1e). The judgment for the formation of the nanoparticle networks can be found in section 4 of the Supporting Information. The nanoparticle networks formed by the A_4B_2-*g*-NPs are honeycomb-like networks, while the A_3B_3-*g*-NPs self-assemble into kagomé networks. The kagomé network is a trihexagonal tiling pattern and has shown high functional properties.[33−35] From Figure 1f, it is observed that the A_4B_2 diblock copolymer-grafted nanoparticles are arranged into a six-coordinated lattice with defects. It should be noted that the highly ordered nanoparticle networks obtained in the $A_{6-n}B_n$-*g*-NP/AC mixtures are rarely observed in homopolymer/nanoparticle systems. Our simulation results, given in section 5 of the Supporting Information, indicate that the $A_{6-n}B_n$-*g*-NPs in the homopolymers tend to form low-order networks.

Figure 1b−f shows that the arrangement order of the BNPs is higher than that of the homopolymer-grafted nanoparticles. We use an arrangement order parameter based on the distribution of angles (θ) formed by three neighboring nanoparticles to quantify the arrangement order.[36] The definition of θ is provided in the inset of Figure 1g. The arrangement order parameter is defined as the ratio of the number of angles distributed within a small angle ($\pm 5°$) around the characteristic angles relative to the total number of angles. The values of the arrangement order parameter are shown in Figure 1g. The homopolymer-grafted nanoparticles are arranged in a disordered manner and exhibit a low arrangement order parameter smaller than 0.4. When the grafted homopolymers are replaced with block copolymers, the nanoparticles are arranged into ordered nanostructures. As seen in Figure 1g, the arrangement order parameter first increases and then decreases with increasing number of B beads. The formation of ordered nanoparticle aggregations can be attributed to the confinement of the nanoparticles in the A domains, which can be characterized in terms of the distance between the nanoparticles and the center of the A domains (D_{PC}). As shown in Figure 1h, D_{PC} decreases with increasing graft composition. This indicates that the block copolymer-grafted nanoparticles prefer to concentrate at the center of the A domains.

The difference in the nanoparticle assembly between the A homopolymer-grafted nanoparticles and the AB block copolymer-grafted nanoparticles in the matrix formed by the AC block copolymer can be rationalized by considering the entropic contributions. To gain detailed insight into the entropic contribution, we considered the excess entropy defined as the difference between the thermodynamic entropy and the entropy of the ideal gas under the same temperature and density conditions.[37] Details of the calculations of the excess entropy are provided in section 2 of the Supporting Information. Figure 2 shows the excess entropy per bead of the A blocks (S_{AA}) in the AC block copolymers that form the matrix. As seen, S_{AA} increases significantly when the grafted homopolymers are replaced by the block copolymers, which indicates that the entropy of A blocks plays an important role in the formation of ordered organization of the block copolymer-grafted nanoparticles. The increase in the S_{AA} of the AB-*g*-NP/AC diblock copolymer mixtures can be attributed to the formation of nanoparticle clusters. While homopolymer-grafted nanoparticles are dispersed uniformly in the A domains, the diblock copolymer-grafted nanoparticles prefer to aggregate and form clusters. As nanoparticle clusters

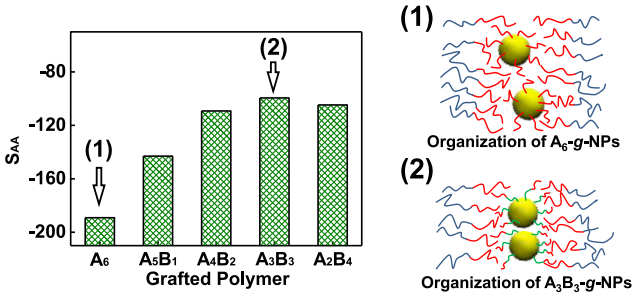

Figure 2. Excess entropy per bead S_{AA} calculated from the pair correlation function between the A beads of AC block copolymers in the nanostructures formed by $A_{6-n}B_n$-*g*-NP/AC.

are formed, the A blocks tend to be stretched, which would increase the free energy. To alleviate this effect, the stretching of A blocks is weakened by the segregation of the grafted nanoparticles into the very center of A domains (see Figure 1h), which leads to an increase in the entropy S_{AA} and decreases the free energy.

We then consider the effect of the nanoparticle concentration φ_P on the nanoparticle arrangement in the $A_{6-n}B_n$-*g*-NP/AC mixtures at different graft compositions f_B. We consider nanoparticle concentrations not higher than 0.05 so that the mixtures self-assemble into lamellar nanostructures. The nanoparticle concentration significantly influences the organization of the nanoparticles. As seen in Figure 3a, the arrangement order parameter first increases and then decreases with increasing φ_P for all $A_{6-n}B_n$-*g*-NP/AC mixtures at different values of f_B. The location of the grafted nanoparticles is also dependent on the nanoparticle concentration, as shown in Figure 3b. For homopolymer-grafted nanoparticles (A_6-*g*-NPs), the distance between the nanoparticles and the center of the A domains (D_{PC}) increases significantly with increasing φ_P. For block copolymer-grafted nanoparticles, D_{PC} changes slightly first and then increases substantially with increasing φ_P. The relation between the nanostructures of the $A_{6-n}B_n$-*g*-NP/AC and the φ_P/f_B is summarized in Figure S4. It is shown that the block copolymer-grafted nanoparticles first form disordered aggregates and then arrange into ordered nanostructures when φ_P increases from 0.02 to 0.04. Upon further increasing the φ_P to 0.045 and 0.05, the block copolymer-grafted nanoparticles assemble into less ordered nanostructures.

Dielectric Properties of the Self-Assembled Nanostructures. The dielectric properties of polymer composites are important for their applications in optical devices, electronic devices, and energy storage. In this subsection, by combining CGMD and finite difference quasielectrostatic modeling, we investigate the correlation between the macroscopic effective permittivity and the self-assembled nanostructures. The nanostructures obtained from the CGMD simulations serve as the input for finite difference quasielectrostatic modeling. Finite difference quasielectrostatic modeling is employed to examine the permittivity of the mixture systems. The permittivity of the nanoparticles and polymers are taken from ref 9. The real and imaginary parts of the permittivities for the nanoparticles are respectively set to be 1235 and 150, i.e., $\varepsilon_n = 1235 - j150$. For the polymers, the real and imaginary parts of the permittivities are respectively set to be 3.6 and 0.8, i.e., $\varepsilon_p = 3.6 - j0.8$. We consider the permittivity (ε_z) along the direction parallel to the lamellae formed by the

https://doi.org/10.1021/acs.nanolett.1c00122
Nano Lett. 2021, 21, 2982−2988

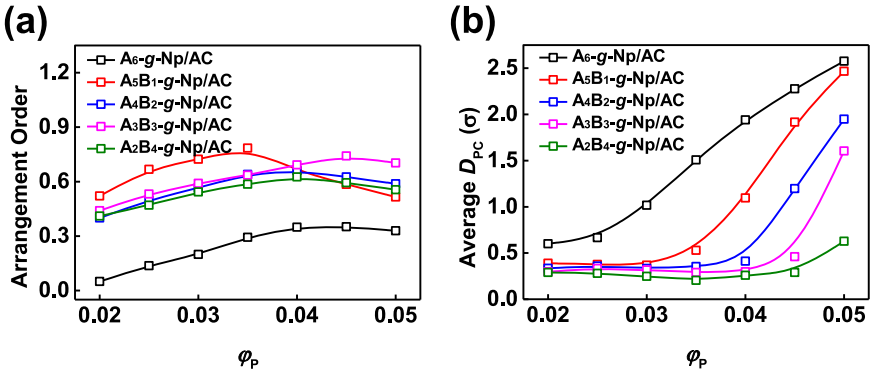

Figure 3. Plots of the arrangement order parameter (a) and average D_{PC} (b) as a function of nanoparticle concentration φ_P in nanostructures formed by the $A_{6-n}B_n$-*g*-NP/AC at various *n*.

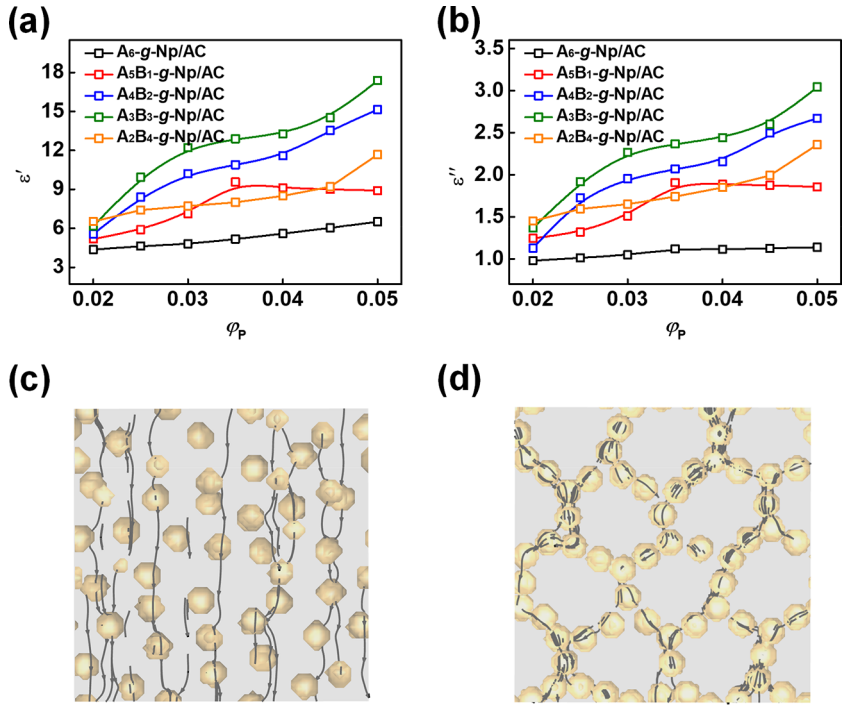

Figure 4. Plots of the real part (a) and imaginary part (b) of permittivity for the $A_{6-n}B_n$-*g*-NP/AC systems as a function of the nanoparticle concentration. The electric field lines around the nanoparticles in the A_6-*g*-NP/AC (c) and A_3B_3-*g*-NP/AC (d) systems at φ_P = 0.04.

block copolymers. Therefore, an external electric field parallel to the lamellae is applied to evaluate ε_z. More details about the simulation method can be found in section 3 of the Supporting Information.

Figure 4 shows the permittivities for the nanostructures of the $A_{6-n}B_n$-*g*-NP/AC mixtures with φ_P varying from 0.02 to 0.05. The real part of the effective permittivity of the nanostructures formed by the A_6-*g*-NP/AC systems increases slightly with increasing φ_P. However, for the A_5B_1-*g*-NP/AC mixtures, a significant increase in the effective permittivity is observed when φ_P increases from 0.02 to 0.035 and a decrease is followed with a further increase in φ_P. The highest permittivity at φ_P = 0.035 can be attributed to the highly ordered nanoparticle stripes formed by the A_5B_1-*g*-NPs. The lower permittivity at higher φ_P is a result of the dramatic decrease in the arrangement order of the A_5B_1-*g*-NPs (see Figure 3a). For the A_4B_2-*g*-NP/AC and A_3B_3-*g*-NP/AC systems, which form hierarchical nanostructures with ordered nanoparticle networks, the effective permittivities also increase significantly with increasing φ_P. Additionally, the permittivities of the two systems are much higher than those of the A_6-*g*-NP/AC, A_5B_1-*g*-NP/AC, and A_2B_4-*g*-NP/AC systems. The evolution of the imaginary part of the permittivity for the mixtures as a function of nanoparticle concentration is similar to the real part, as shown in Figure 4b.

To understand the physical mechanisms of the significant improvement in the permittivities of the hierarchical nanostructures with ordered nanoparticle networks, we analyzed the distribution of electric field in the nanostructures self-assembled from A_6-*g*-NP/AC and A_3B_3-*g*-NP/AC mixtures at φ_P = 0.04. Since the distinction in the permittivity of these structures is a result of the differences in the nanoparticle arrangement, we focus on the electric field around the nanoparticles. As shown in Figure 4c, the electric field lines are almost straight in the A_6-*g*-NP/AC mixtures, which indicates that the random arrangement of nanoparticles has less influence on the electric field. In contrast, the electric field lines in the nanostructures formed by the A_3B_3-*g*-NP/AC

https://doi.org/10.1021/acs.nanolett.1c00122
Nano Lett. 2021, 21, 2982−2988

mixtures are dramatically bent and concentrated around the nanoparticle networks (see Figure 4d). This indicates that the ordered and connected nanoparticle networks provide conductive and bending pathways for electric fields. A concentrated electric field means a high electric field near the nanoparticles, which leads to a high effective permittivity of the hierarchical nanostructures with ordered nanoparticle networks. The distribution of the electric field lines in the A_4B_2-*g*-NP/AC systems with ordered nanoparticle networks is similar to that of the A_3B_3-*g*-NP/AC systems, while the arrangement of the A_5B_1-*g*-NPs and A_2B_4-*g*-NPs in the matrix formed by the AC block copolymers has less effect on the electric field (see Figure S5).

So far, there is no direct experimental study demonstrating the enhanced permittivity of BNP/BCP mixtures with ordered nanoparticle networks. However, our prediction can be supported by some experimental evidence from works on mixtures of homopolymers and nanoparticles. Recently, Luo et al. constructed a three-dimensional $BaTiO_3$ (BT) nanoparticle network in polymer nanocomposites which exhibited much higher permittivity than the ones with uniformly dispersed $BaTiO_3$ nanoparticles.[9] The networks formed by the $BaTiO_3$ nanoparticles are percolation networks, and the percolation threshold f_c is about 25%. The permittivity grows relatively slowly with the f_{BT} lower than 25%, while the 3D-BT network is not fully formed throughout the entire system, as shown in Figure 5. As the nanoparticle concentration further increases

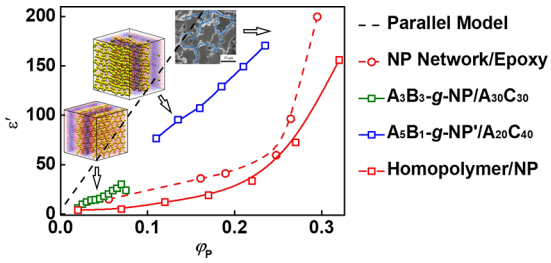

Figure 5. Plots of the real part of permittivity as a function of the nanoparticle concentration in the nanostructures formed by the mixtures in our simulations and Luo's experiments measured at 1 kHz. The black dash line denotes the effective permittivity of polymer composites predicted by the parallel model. The inserts show the representative nanostructures for the corresponding systems. The blue lines in the inset of the SEM image are visual guides to observe the nanoparticle network. The experimental results are reproduced with permission from ref 9. Copyright 2017, The Royal Society of Chemistry.

and approaches 25%, the 3D network of BT becomes more complete and extends throughout the epoxy matrix, which results in a sharp increase in the permittivity. To simulate the enhancement effect of the formation of the nanoparticle networks on the permittivity, we construct a model of polymer/nanoparticle mixture system that can form percolation nanoparticle networks driven by the depletion effect. The details for the model system can be found in section 8 of Supporting Information. The percolation threshold for the model system of polymer/nanoparticle mixtures is about 0.1 (see Figure S6). For the permittivity of the polymer/nanoparticle mixtures, we also observe that the dielectric properties change sharply after the network formation at $\varphi_P > 0.1$, as shown in Figure 5. The evolution of the permittivity with increasing φ_P is in qualitative agreement with the experimental observation in Luo's work.

Beyond reproducing some experimental results, we propose a new strategy of using BNPs to construct ordered nanoparticle organization in the block copolymer matrix. By tuning the graft composition and nanoparticle concentration of the $A_{6-n}B_n$-*g*-NP/AC mixtures, a series of hierarchical hybrid nanostructures with ordered nanoparticle strips and networks are observed. It is revealed that the nanoparticle ordering in these mixtures is an entropy-driven process. The formation of highly ordered nanoparticle networks in hierarchical nanostructures gives rise to high permittivity (see Figure 5). For the mixture of A_3B_3-*g*-NP/$A_{30}C_{30}$, the self-assembled nanostructure remains as the lamellae with ordered nanoparticle networks, and the permittivity grows to 30 as the filler loading increases to 7%, as shown in Figure 5. When the filler loading increases to 7.5%, the perforated lamellae with less ordered nanoparticle network is formed and the permittivity decreases. This means, for the A_3B_3-*g*-NP/$A_{30}C_{30}$ systems, the maximum filler loading to keep the ordered nanostructures is about 7% with a permittivity of ∼30. The maximum filler loading to keep the ordered nanostructures can be increased via the molecular design of the AC block copolymers or AB-*g*-NPs. For example, we change the block copolymer of $A_{30}C_{30}$ to $A_{20}C_{40}$ and change the A_3B_3-*g*-NP to A_5B_1-*g*-NP′ with nanoparticle diameter of 4.5σ. The mixtures of such A_5B_1-*g*-NP′/$A_{20}C_{40}$ form the lamellae with nanoparticle networks at higher nanoparticle loading above 20%, and the permittivity increases to ∼170. It should be noted that the previously reported permittivities of nanoparticle filled composites are much lower than the values predicted by the parallel model (an ideal model, a linear summation of the permittivities of nanoparticles and matrix).[9] Our simulation results indicate that, through the molecular design of the AB-*g*-NPs and AC block copolymers, the effective permittivity of the self-assembled nanostructures gets closer to the values predicted by the parallel model.

In summary, we developed a multiscale approach coupling CGMD simulation with finite difference quasielectrostatic modeling to investigate the self-assembled nanostructures and dielectric properties of AB-*g*-NP and AC block copolymer mixtures. In the mixtures, the block copolymer-grafted nanoparticles self-assemble into ordered stripes or networks. The ordered and connected nanoparticle networks, including the honeycomb-like and kagomé networks, significantly improve the permittivity of the self-assembled nanostructures. The multiscale approach is useful for understanding the relation between the nanostructures and permittivity of the polymer/NP systems. The results may provide guidance for preparing advanced functional nanocomposites with high permittivity.

■ ASSOCIATED CONTENT

Supporting Information

The Supporting Information is available free of charge at https://pubs.acs.org/doi/10.1021/acs.nanolett.1c00122.

Details regarding the model and method; judgment for the formation of nanoparticle networks; nanostructures self-assembled from the $A_{6-n}B_n$-*g*-NP/homopolymer mixtures; effect of the nanoparticle concentration on the self-assembled nanostructures of the $A_{6-n}B_n$-*g*-NP/AC mixtures; electric field lines in the A_5B_1-*g*-NP/AC, A_4B_2-*g*-NP/AC and A_2B_4-*g*-NP/AC mixtures; and

https://doi.org/10.1021/acs.nanolett.1c00122
Nano Lett. 2021, 21, 2982−2988

percolation nanoparticle networks formed by polymer/nanoparticle mixtures (PDF)

AUTHOR INFORMATION

Corresponding Author

Jiaping Lin − *Shanghai Key Laboratory of Advanced Polymeric Materials, Key Laboratory for Ultrafine Materials of Ministry of Education, Frontiers Science Center for Materiobiology and Dynamic Chemistry, School of Materials Science and Engineering, East China University of Science and Technology, Shanghai 200237, China;* orcid.org/0000-0001-9633-4483; Email: jlin@ecust.edu.cn

Authors

Zhanwen Xu − *Shanghai Key Laboratory of Advanced Polymeric Materials, Key Laboratory for Ultrafine Materials of Ministry of Education, Frontiers Science Center for Materiobiology and Dynamic Chemistry, School of Materials Science and Engineering, East China University of Science and Technology, Shanghai 200237, China*

Liangshun Zhang − *Shanghai Key Laboratory of Advanced Polymeric Materials, Key Laboratory for Ultrafine Materials of Ministry of Education, Frontiers Science Center for Materiobiology and Dynamic Chemistry, School of Materials Science and Engineering, East China University of Science and Technology, Shanghai 200237, China;* orcid.org/0000-0002-0182-7486

Liquan Wang − *Shanghai Key Laboratory of Advanced Polymeric Materials, Key Laboratory for Ultrafine Materials of Ministry of Education, Frontiers Science Center for Materiobiology and Dynamic Chemistry, School of Materials Science and Engineering, East China University of Science and Technology, Shanghai 200237, China;* orcid.org/0000-0002-5141-8584

Complete contact information is available at: https://pubs.acs.org/10.1021/acs.nanolett.1c00122

Notes

The authors declare no competing financial interest.

ACKNOWLEDGMENTS

This work was supported by the National Natural Science Foundation of China (Grants 51833003, 51621002, and 21975073).

REFERENCES

(1) Chen, J.; Guo, H.; He, X.; Liu, G.; Xi, Y.; Shi, H.; Hu, C. Enhancing performance of triboelectric nanogenerator by filling high dielectric nanoparticles into sponge pdms film. *ACS Appl. Mater. Interfaces* **2016**, *8*, 736−744.

(2) Seung, W.; Yoon, H.-J.; Kim, T. Y.; Ryu, H.; Kim, J.; Lee, J.-H.; Lee, J. H.; Kim, S.; Park, Y. K.; Park, Y. J.; Kim, S.-W. Boosting power-generating performance of triboelectric nanogenerators via artificial control of ferroelectric polarization and dielectric properties. *Adv. Energy Mater.* **2017**, *7*, 1600988.

(3) Shi, G.; Hanlumyuang, Y.; Liu, Z.; Gong, Y.; Gao, W.; Li, B.; Kono, J.; Lou, J.; Vajtai, R.; Sharma, P.; Ajayan, P. M. Boron nitride-graphene nanocapacitor and the origins of anomalous size-dependent increase of capacitance. *Nano Lett.* **2014**, *14*, 1739−1744.

(4) Tang, H.; Sodano, H. A. Ultra high energy density nanocomposite capacitors with fast discharge using $Ba_{0.2}Sr_{0.8}TiO_3$ nanowires. *Nano Lett.* **2013**, *13*, 1373−1379.

(5) Silibin, M. V.; Belovickis, J.; Svirskas, S.; Ivanov, M.; Banys, J.; Solnyshkin, A. V.; Gavrilov, S. A.; Varenyk, O. V.; Pusenkova, A. S.; Morozovsky, N.; Shvartsman, V. V.; Morozovska, A. N. Polarization reversal in organic-inorganic ferroelectric composites: Modeling and experiment. *Appl. Phys. Lett.* **2015**, *107*, 142907.

(6) Xu, Y.; Swaans, E.; Chen, S.; Basak, S.; Harks, P. P. R. M. L.; Peng, B.; Zandbergen, H. W.; Borsa, D. M.; Mulder, F. M. A high-performance Li-ion anode from direct deposition of Si nanoparticles. *Nano Energy* **2017**, *38*, 477−485.

(7) Zhang, X.; Shen, Y.; Zhang, Q.; Gu, L.; Hu, Y.; Du, J.; Lin, Y.; Nan, C.-W. Ultrahigh energy density of polymer nanocomposites containing $BaTiO_3$@TiO_2 nanofibers by atomic-scale interface engineering. *Adv. Mater.* **2015**, *27*, 819−824.

(8) Feng, Y.; Liang, P.; Tang, B.; Wang, Y.; Liu, J.; Shui, L.; Li, H.; Tian, M.; Zhang, L.; Zhou, G. Construction of particle network for ultrahigh permittivity of dielectric polymer composite toward energy devices: A molecular dynamics study. *Nano Energy* **2019**, *64*, 103985.

(9) Luo, S.; Shen, Y.; Yu, S.; Wan, Y.; Liao, W.-H.; Sun, R.; Wong, C.-P. Construction of a 3D-$BaTiO_3$ network leading to significantly enhanced dielectric permittivity and energy storage density of polymer composites. *Energy Environ. Sci.* **2017**, *10*, 137−144.

(10) Liu, Z.; Xu, Z.; Wang, L.; Lin, J. Distinctive optical properties of hierarchically ordered nanostructures self-assembled from multiblock copolymer/nanoparticle mixtures. *Macromol. Rapid Commun.* **2020**, *41*, 2000131.

(11) Zhang, L.; Lin, J. Hierarchically ordered nanocomposites self-assembled from linear-alternating block copolymer/nanoparticle mixture. *Macromolecules* **2009**, *42*, 1410−1414.

(12) Zhang, Q.; Zhang, L.; Lin, J. Percolating behavior of nanoparticles in block copolymer host: Hybrid particle-field simulations. *J. Phys. Chem. C* **2017**, *121*, 23705−23715.

(13) Bai, P.; Yang, S.; Bao, W.; Kao, J.; Thorkelsson, K.; Salmeron, M.; Zhang, X.; Xu, T. Diversifying nanoparticle assemblies in supramolecule nanocomposites via cylindrical confinement. *Nano Lett.* **2017**, *17*, 6847−6854.

(14) Huang, J.; Qian, Y.; Evans, K.; Xu, T. Diffusion-dependent nanoparticle assembly in thin films of supramolecular nanocomposites: Effects of particle size and supramolecular morphology. *Macromolecules* **2019**, *52*, 5801−5810.

(15) Lin, Y.; Daga, V. K.; Anderson, E. R.; Gido, S. P.; Watkins, J. J. Nanoparticle-driven assembly of block copolymers: A simple route to ordered hybrid materials. *J. Am. Chem. Soc.* **2011**, *133*, 6513−6516.

(16) Xu, C.; Ohno, K.; Ladmiral, V.; Composto, R. J. Dispersion of polymer-grafted magnetic nanoparticles in homopolymers and block copolymers. *Polymer* **2008**, *49*, 3568−3577.

(17) Pang, X.; He, Y.; Jiang, B.; Iocozzia, J.; Zhao, L.; Guo, H.; Liu, J.; Akinc, M.; Bowler, N.; Tan, X.; Lin, Z. Block copolymer/ferroelectric nanoparticle nanocomposites. *Nanoscale* **2013**, *5*, 8695−8702.

(18) He, J.; Huang, X.; Li, Y.-C.; Liu, Y.; Babu, T.; Aronova, M. A.; Wang, S.; Lu, Z.; Chen, X.; Nie, Z. Self-assembly of amphiphilic plasmonic micelle-like nanoparticles in selective solvents. *J. Am. Chem. Soc.* **2013**, *135*, 7974−7984.

(19) He, J.; Liu, Y.; Babu, T.; Wei, Z.; Nie, Z. Self-assembly of inorganic nanoparticle vesicles and tubules driven by tethered linear block copolymers. *J. Am. Chem. Soc.* **2012**, *134*, 11342−11345.

(20) Lin, X.; Ye, S.; Kong, C.; Webb, K.; Yi, C.; Zhang, S.; Zhang, Q.; Fourkas, J. T.; Nie, Z. Polymeric ligand-mediated regioselective bonding of plasmonic nanoplates and nanospheres. *J. Am. Chem. Soc.* **2020**, *142*, 17282−17286.

(21) Liu, Y.; Liu, Y.; Yin, J.-J.; Nie, Z. Self-assembly of amphiphilic block copolymer-tethered nanoparticles: A new approach to nanoscale design of functional materials. *Macromol. Rapid Commun.* **2015**, *36*, 711−725.

(22) Mai, Y.; Eisenberg, A. Controlled incorporation of particles into the central portion of block copolymer rods and micelles. *Macromolecules* **2011**, *44*, 3179−3183.

(23) Leffler, V. B.; Mayr, L.; Paciok, P.; Du, H.; Dunin-Borkowski, R. E.; Dulle, M.; Förster, S. Controlled assembly of block copolymer coated nanoparticles in 2D arrays. *Angew. Chem., Int. Ed.* **2019**, *58*, 8541−8545.

(24) Li, X.; Gu, M.; Zhang, L.; Lin, J. Computational investigation on the superstructures of micelles from amphiphilic DNA block copolymers. *Acta Polym. Sin.* **2020**, *51*, 1257−1266.
(25) Gu, J.; Zhang, R.; Zhang, L.; Lin, J. Harnessing zone annealing to program directional motion of nanoparticles in diblock copolymers: Creating periodically well-ordered nanocomposites. *Macromolecules* **2020**, *53*, 2111−2122.
(26) Xu, Z.; Lin, J.; Zhang, L.; Tian, X.; Wang, L. Modulation of molecular orientation enabling high photovoltaic performance of block copolymer nanostructures. *Mater. Chem. Front.* **2019**, *3*, 2627−2636.
(27) Zhong, S.; Dang, Z.; Zha, J. Prediction on effective permittivity of 0-3 connectivity particle/polymer composites at low concentration with finite element method. *IEEE Trans. Dielectr. Electr. Insul.* **2018**, *25*, 2122−2128.
(28) Thompson, R. B.; Ginzburg, V. V.; Matsen, M. W.; Balazs, A. C. Predicting the mesophases of copolymer-nanoparticle composites. *Science* **2001**, *292*, 2469.
(29) Gao, K.; Wan, H.; Tsen, E. J. L.; Liu, J.; Lyulin, A. V.; Zhang, L. Unveiling the mechanism of the location of the grafted nanoparticles in a lamellar-forming block copolymer. *Langmuir* **2020**, *36*, 194−203.
(30) Calame, J. P. Finite difference simulations of permittivity and electric field statistics in ceramic-polymer composites for capacitor applications. *J. Appl. Phys.* **2006**, *99*, 084101.
(31) Myroshnychenko, V.; Brosseau, C. Finite-element method for calculation of the effective permittivity of random inhomogeneous media. *Phys. Rev. E* **2005**, *71*, 016701.
(32) Hardin, R. H.; Sloane, N. J. A.; Smith, W. D. Tables of spherical codes with icosahedral symmetry. 2000. http://NeilSloane.com/icosahedral.codes/ (accessed January 10, 2021).
(33) Mallory, S. A.; Cacciuto, A. Activity-enhanced self-assembly of a colloidal kagome lattice. *J. Am. Chem. Soc.* **2019**, *141*, 2500−2507.
(34) Chen, Q.; Bae, S. C.; Granick, S. Directed self-assembly of a colloidal kagome lattice. *Nature* **2011**, *469*, 381−384.
(35) Pan, H.; Han, Y.; Li, J.; Zhang, H.; Du, Y.; Tang, N. Half-metallicity in a honeycomb−kagome-lattice mg3c2 monolayer with carrier doping. *Phys. Chem. Chem. Phys.* **2018**, *20*, 14166−14173.
(36) Chao, H.; Riggleman, R. A. Inverse design of grafted nanoparticles for targeted self-assembly. *Mol. Syst. Des. Eng.* **2018**, *3*, 214−222.
(37) Dong, B.; Huang, Z.; Chen, H.; Yan, L.-T. Chain-stiffness-induced entropy effects mediate interfacial assembly of janus nanoparticles in block copolymers: From interfacial nanostructures to optical responses. *Macromolecules* **2015**, *48*, 5385−5393.

https://doi.org/10.1021/acs.nanolett.1c00122
Nano Lett. 2021, 21, 2982−2988